THE JOURNAL OF BIOLOGICAL CHEMISTRY VOL. 288, NO. 8, pp. 5268–5277, February 22, 2013

Type I Phosphotidylinosotol 4-Phosphate 5-Kinase γ Regulates Osteoclasts in a Bifunctional Manner*[S]

Received for publication, December 17, 2012 Published, JBC Papers in Press, January 8, 2013, DOI 10.1074/jbc.M112.446054

Tingting Zhu[‡], Jean C. Chappel[‡], Fong-Fu Hsu[§], John Turk[§], Rajeev Aurora[¶], Krzysztof Hyrc[‖], Pietro De Camilli[**], Thomas J. Broekelmann[‡‡], Robert P. Mecham[‡‡], Steven L. Teitelbaum[‡§1], and Wei Zou[‡2]

From the [‡]Department of Pathology and Immunology, [§]Department of Medicine, [‡‡]Department of Cell Biology and Physiology, [‖]Center for the Investigation of Membrane Excitability Diseases, Washington University in St. Louis School of Medicine, St. Louis, Missouri 63110, the [¶]Department of Molecular Microbiology and Immunology, St. Louis University School of Medicine, St. Louis, Missouri 63104, and the [**]Department of Cell Biology and Howard Hughes Medical Institute, Yale University, New Haven, Connecticut 06520

Background: $PI(4,5)P_2$, mainly synthesized by PIP5KIγ, is essential for normal cell function.
Results: Deficiency or overexpression of PIP5KIγ, which results in decrease or increase of $PI(4,5)P_2$, respectively, impairs osteoclast differentiation and function.
Conclusion: Optimal PIP5KIγ and $PI(4,5)P_2$ expression are important for osteoclast function.
Significance: This is the first demonstration that PIP5KIγ regulates cells in a bifunctional manner.

Type 1 phosphotidylinosotol-4 phosphate 5 kinase γ (PIP5KIγ) is central to generation of phosphotidylinosotol (4,5)P_2 ($PI(4,5)P_2$). PIP5KIγ also participates in cytoskeletal organization by delivering talin to integrins, thereby enhancing their ligand binding capacity. As the cytoskeleton is pivotal to osteoclast function, we hypothesized that absence of PIP5KIγ would compromise their resorptive capacity. Absence of the kinase diminishes PI(4,5) abundance and desensitizes precursors to RANK ligand-stimulated differentiation. Thus, PIP5KI$\gamma^{-/-}$ osteoclasts are reduced in number *in vitro* and confirm physiological relevance *in vivo*. Despite reduced numbers, PIP5KI$\gamma^{-/-}$ osteoclasts surprisingly have normal cytoskeletons and effectively resorb bone. PIP5KIγ overexpression, which increases $PI(4,5)P_2$, also delays osteoclast differentiation and reduces cell number but in contrast to cells lacking the kinase, its excess disrupts the cytoskeleton. The cytoskeleton-disruptive effects of excess PIP5KIγ reflect its kinase activity and are independent of talin recognition. The combined arrested differentiation and disorganized cytoskeleton of PIP5KIγ-transduced osteoclasts compromises bone resorption. Thus, optimal PIP5KIγ and $PI(4,5)P_2$ expression, by osteoclasts, are essential for skeletal homeostasis.

Bone resorption is the unique purview of the osteoclast. It involves cytoskeletal organization to polarize vesicles toward the bone-apposed plasma membrane into which they insert to deliver their cargo of matrix-degrading molecules to the extracellular, resorptive microenvironment (1). As phosphatidylinositols (PIs)[3] are key to cytoskeletal organization and function of all mammalian cells, it is likely that they participate in the bone resorptive process (2, 3).

$PI(4,5)P_2$ is among the most biologically relevant PIs as it modulates phenomena such as migration, apoptosis, and cell division (4, 5). A key event in the biological activity of $PI(4,5)P_2$ is its metabolism by phospholipase Cγ into diacylglycerol and inositol-1,4,5-trisphosphate which, via ionized calcium, activates nuclear factor of activated T cells c1 (NFATc1) for osteoclast differentiation (4–6). In consequence, arrest of $PI(4,5)P_2$ metabolism by deletion of phospholipase Cγ2, the relevant isoform in the resorptive cell, inhibits osteoclastogenesis (7). $PI(4,5)P_2$ also regulates osteoclast cytoskeletal organization by interacting with gelsolin and WASP to control podosome signaling and formation of actin rings which isolate the resorptive milieu from the general extracellular space (3). However, phospholipase Cγ2 deletion, which presumably increases $PI(4,5)P_2$ by preventing its metabolism, blunts the capacity of the cell to organize its cytoskeleton via the $\alpha v\beta 3$ integrin and thus degrades bone (8, 9).

$PI(4,5)P_2$ is principally synthesized by phosphorylation of phosphatidylinositol-4 phosphate at the 5-position of the inositol ring via type I phosphatidylinositol 4-phosphate 5 kinase (PIP5KI). Three PIP5KI isoforms, α, β, and γ, with conserved catalytic domains, are in hand. These isoforms enjoy discrete biological activities likely dictated by their non-overlapping distributions, reflecting, in turn, their distinct C-terminal regions.

* This work was supported, in whole or in part, by National Institutes of Health Grants AR032788, AR046523, AR054618, AR057037, and AR057235 (to S. L. T.), HL53325 and HL74138 (to R. P. M.), and NS036251 (to P. D. C.). This work was also supported by NIH Grants P41-RR-00954, P60-DK-20579, and P30-DK56341.

[S] This article contains supplemental Table S1, Figs. 1 and 2, and Movies 1 and 2.

[1] To whom correspondence may be addressed: Dept. of Pathology and Immunology, Washington University in St. Louis School of Medicine, Campus Box 8118, 660 S. Euclid Ave., St. Louis, MO. Tel.: 314-454-8463; Fax: 314-454-5505; E-mail: teitelbs@wustl.edu.

2 To whom correspondence may be addressed: Dept. of Pathology and Immunology, Washington University in St. Louis School of Medicine, Campus Box 8118, 660 S. Euclid Ave., St. Louis, MO. Tel.: 314-454-7353; Fax: 314-454-5505; E-mail: weizou@wustl.edu.

[3] The abbreviations used are: PI, phosphatidylinositol; PIP5KIγ, type 1 phosphotidylinosotol-4 phosphate 5 kinase γ; RANKL, receptor activator of NFκB ligand; NFATc1, nuclear factor of activated T cells c1; TRAP, tartrate-resistant acid phosphatase; KD, kinase-inactive; MEM, minimum essential medium.

For example, PIP5KIα targets membrane ruffles, whereas PIP5KIβ manifests a perinuclear distribution (4).

PIP5KIγ represents at least three splice variants, with the two most studied being PIP5KIγ1 (PIP5KIγ-87), consisting of 635 amino acids, and PIP5KIγ2 (PIP5KIγ-90) with an additional 26 residue C-terminal extension (4, 10). Differential immunostaining of the two species establish PIP5KIγ1 resides diffusely within the cytoplasm, whereas PIP5KIγ2 targets focal adhesions, suggesting it participates in cytoskeletal organization (11–14). In addition to its enzymatic activity, PIP5KIγ2 binds talin and delivers it to β integrin subunits. Upon talin association, the α/β heterodimers undergo conformational change to increase affinity for matrix-residing ligand. PIP5KIγ2 may also enhance β-integrin/talin association by local generation of $PI(4,5)P_2$.

Talin promotes the capacity of osteoclasts to organize their cytoskeleton and thus resorb bone (15). Moreover, bone resorption is an exocytic process, which PIP5KIγ regulates in other cells, and we find the kinase is expressed with differentiation of osteoclast precursors into the resorptive polykaryon (11, 16–18). We find absence of PIP5KIγ delays osteoclast differentiation in response to receptor activator of NFκB ligand (RANKL) but once formed, the cells exhibit no cytoskeletal or functional abnormalities. In keeping with these *in vitro* observations, PIP5KI$\gamma^{-/-}$ mice have arrested osteoclastogenesis *in vivo*. Surprisingly, excess PIP5KIγ also delays osteoclast differentiation and in contrast to deficiency of the kinase, disrupts the cytoskeleton of the osteoclast in a talin-independent manner. Thus, reflecting abundance, PIP5KIγ exerts varied effects on osteoclasts.

EXPERIMENTAL PROCEDURES

Mice—PIP5KI$\gamma^{+/-}$ (C57/BL6 background) mice were described previously (15). Mice were genotyped by PCR using 5′-GCCTCACAGAGATTTGACCTGTCA-3′ (PIP5Kγ^{+}) and 5′-CACCCCTTCCCAGCCTCTGA-3′ (PIP5Kγ^{-}) as forward primers in combination with the 5′-CCTCACATCCTGCTCACTCAGGACC-3′ reverse primer. The products (250 and 650 bp for PIP5Kγ^{-} and PIP5Kγ^{+}, respectively) were resolved on a 1% agarose gel. PIP5K$\gamma^{-/-}$ and WT liver cells were obtained from postnatal day 0 pups and prepared as described (19). Animals were housed in the animal care unit of the Washington University School of Medicine and were maintained according to guidelines of the Association for Assessment and Accreditation of Laboratory Animal Care. All animal experimentation was approved by the Animal Studies Committee of the Washington University School of Medicine.

Reagents—Recombinant M-CSF was obtained from R&D Systems (Minneapolis, MN). Glutathione *S*-transferase (GST)-RANKL was expressed in our laboratory as described (20) and unless specified used at 100 ng/ml. The sources of antibodies were as follows: rabbit anti-HA polyclonal antibody was from Covance (Emeryville, CA); antiphosphotyrosine mAb 4G10 (p-Tyr) was from Upstate (Charlottesville, VA); directed against the Src protein were gifts from Andrey Shaw (Department of Pathology, Washington University School of Medicine, St Louis, MO); mouse anti-NFATc1 antibody was from Santa Cruz Biotechnology (Santa Cruz, CA); rabbit anti-β3-integrin antibody, JNK, p-JNK, p38, p-p38, Akt, p-Akt, ERK, p-ERK, IκB, and p-IκB were from Cell Signaling (Beverly, MA); mouse anti-talin monoclonal and anti-actin antibodies were from Sigma; mouse anti-PIP5Kγ was from BD Biosciences; rabbit anti-PIP5Kγ-pan and anti-PIP5Kγ2 were for immunoblot (21); rabbit anti-PIP5Kγ-pan WI155 for immunostaining was kindly provided by Dr. Anderson (14). All other chemicals were obtained from Sigma.

Macrophage Isolation and Osteoclast Culture—Primary liver and bone marrow macrophages were obtained and treated as described to generate osteoclasts (19, 20). Cells were extracted with α-MEM and cultured in α-MEM containing 10% inactivated FBS, 100 international units/ml penicillin, and 100 μg/ml streptomycin (α-10 medium) with 1:10 CMG (conditioned medium supernatant containing recombinant M-CSF 1 μg/ml) on Petri dishes (28). Cells were incubated at 37 °C in 6% CO_2 for 4 days and then washed with PBS and lifted with 1× trypsin/EDTA (Invitrogen) in PBS. Unless specified differently, 1.5×10^4 cells were cultured in 500 μl α-MEM containing 10% heat-inactivated FBS with 100 ng/ml GST-RANKL and 1:50 CMG in 48-well tissue culture plates, some of which contained a sterile bone slice. Cells were fixed and stained for tartrate-resistant acid phosphatase (TRAP) activity after 4–5 days in culture using a commercial kit (387-A; Sigma-Aldrich). For preosteoclast generation, 1.5×10^6 bone marrow macrophages (BMMs) were plated per 10-cm tissue culture dish and maintained in 1:50 CMG and 100 ng/ml GST-RANKL for 3 days. Preosteoclasts were lifted with 0.02% EDTA in PBS. For actin ring staining, cells were cultured on a bovine bone slice in the presence of M-CSF and RANKL for 6 days, at which time cells were fixed in 4% PFA, permeabilized in 0.1% Triton X-100, rinsed in PBS, and immunostained with Alexa Fluor 488 phalloidin (Invitrogen). To quantitate resorption lacunae, bone slices were incubated with peroxidase-conjugated wheat germ agglutinin (Sigma) for 1 h and stained with 3,3′-diaminobenzidine (Sigma).

Plasmids and Retroviral Transduction—Wild-type constructs expressing mouse PIP5KIγ1, PIP5KIγ2, and kinase-inactive (KD) mutant were subcloned into the BamHI and XhoI sites of a pMX retroviral vector in which the puromycin resistance sequence was replaced with one coding for blastocidin resistance (18). cDNA was transfected transiently into Plat-E packaging cells using FuGENE 6 transfection reagent (Roche Applied Science). Virus was collected 48 h after transfection. Macrophages were infected with virus for 24 h in the presence of 1:10 CMG and 4 μg/ml polybrene (Sigma). Cells were selected in the presence of CMG and 1 μg/ml blasticidin (Calbiochem) for 3 days before use as osteoclast precursors.

RNA Extraction and Quantitative RT-PCR—RNA from cultured cells was isolated and purified using the RNeasy RNA purification kit (Qiagen, Valencia, CA); RLT lysis buffer was supplemented with β-mercaptoethanol (1%). Purified RNA was treated with DNase I (Invitrogen) before reverse transcription (RT). RT was performed using SuperScript III (Invitrogen), and quantitative PCR was performed using Power SYBR Green Master mix and gene-specific primers (Applied Biosystems, Foster City, CA). The quantitative PCR reaction was performed on an ABI Prism 7000 (Applied Biosystems).

Ca^{2+} Imaging—Shortly before imaging, WT and PIP5KIγ-deficient macrophages were incubated with 3 μM Fura 4-AM (F14201, Invitrogen) for 30 min at 37 °C in α-MEM containing 10 ng/ml M-CSF. The cells were washed and incubated in fresh α-MEM with 10 ng/ml M-CSF 30 min at 37 °C. Ca^{2+} imaging was performed with a 40× objective of an inverted automated wide field epifluorescence DIC microscope (Leica DMIRE2, Leica Microsystems, Wetzlar, Germany). An objective lens heater was used to improve temperature homogeneity. Images (608 × 512 pixels spatial and 12-bit intensity resolution) were recorded with a cooled Retiga 1300 camera (Qimaging, Burnaby, BC, Canada) every 10 s in 2 × 2 binned acquisition mode, using 100–300-ms exposures. Dynamic images were composed using NIH ImageJ software.

Phosphoinosotide Measurement (Sample Preparation)—Lipids were extracted as described previously by Pettitt *et al.* (22). Briefly, three ml of ice-cold $CHCl_3$-MeOH (1:2; v/v) was added to the cell platelets of BMMs. After vigorous vortexing to ensure cell distribution, the samples were incubated on ice for 15 min, and then ice-cold $CHCl_3$ (1 ml) was added, followed by 1 ml of solution containing 1.76% KCl, 100 mM citric acid, 100 mM Na_2HPO_4, 5 mM EDTA, and 5 mM tetrabutyl ammonium hydrogen sulfate (pH 3.6). After mixing, the samples were incubated on ice for 5 min before centrifugation (200 × *g*, 5 min) to complete the phase split. The lower organic phase was transferred into a clean silanized vial and evaporated to dryness under a stream of nitrogen.

Electrospray Ionization Mass Spectrometry (ESI-MS)—Mass spectrometric analyses of phosphatidylinositol phosphates (PIPs) were carried out in the negative-ion mode using a Thermo Scientific (San Jose, CA) LTQ Orbitrap Velos instrument with Xcalibur operating system. The instrument was operated in FT mode with resolution set at 100,000 (at *m*/*z* 400) and scan from 250 to 1000 m/z. The automatic gain control was set to 1×10^6 ions with a maximal injection time of 100 ms, and one microscan was recorded. The lock mass option was enabled, and deprotonated stearic anion ($C_{17}H_{35}CO_2$-; *m*/*z* 283.26425) was used for internal recalibration of the mass spectra. CID was done with a target value of 3000 in the linear ion trap, maximal injection time of 200 ms, collision energy of 20%, Q value of 0.25, and an activation time of 10 ms. The dry lipid extracts containing PIPs were redissolved in 50 μl of 50% CH_3OH/H_2O, vortexed for 1 min, and centrifuged at 13,600 rpm for 3 min. The supernatant was transferred to a silanized tube and an aliquot (5 μl) of the solution was mixed with 5 μl of methanol (with 1% NH_4OH) and loop injected onto the mass spectrometer via a built-in syringe pump, which maintained a continuous flow of 20 μl/min with 80% methanol (with 0.5% NH_4OH). The skimmer was set at ground potential, the electrospray needle was set at 3.0 kV, and temperature of the heated capillary was 250 °C. Mass spectra were accumulated in the profile mode, and spectra were background subtracted.

Western Blotting and Immunoprecipitation—Cultured cells were washed twice with ice-cold PBS and lysed in radioimmune precipitation assay buffer containing 20 mM Tris-HCl, pH 7.5, 150 mM NaCl, 1 mM EDTA, 1 mM EGTA, 1% Triton X-100, 2.5 mM sodium pyrophosphate, 1 mM β-glycerophosphate, 1 mM Na_3VO_4, 1 mM NaF, and 1× protease inhibitor mixture (Roche Applied Science). After incubation on ice for 10 min, cell lysates were clarified by centrifugation at 15,000 rpm for 10 min. Forty micrograms of total lysates were subjected to 8–12% sodium dodecyl sulfate polyacrylamide gel electrophoresis and transferred onto PVDF membranes. Filters were blocked in 0.1% casein in PBS for 1 h and incubated with primary antibodies at 4 °C overnight followed by probing with fluorescence-labeled secondary antibodies (Jackson ImmunoResearch Laboratories). Proteins were detected with the Odyssey Infrared Imaging System (LI-COR Biosciences).

Actin Ring Staining and Bone Resorption Assay—Osteoclasts were generated on bone slices by exposure to 100 ng/ml RANKL and 20 ng/ml M-CSF. For actin ring staining, the cells were fixed in 4% paraformaldehyde and permeablized in 0.1% Triton X-100, rinsed in PBS, and immunostained with Alexa Fluor 488-phalloidin (Invitrogen). For bone resorption assay, osteoclasts were removed, and resorption pits were visualized by incubation of the specimen with 20 μg/ml peroxidase-conjugated wheat germ agglutinin as described previously and stained with 3,3′-diaminobenzidine (Sigma).

Medium CTx-1 Assay—Macrophages were cultured on bone with 100 ng/ml RANKL and 1:50 CMG supernatant for 6 days. Medium (α-10) was changed 1 day before harvesting. Medium CTx-1 concentration was determined using CrossLap for Culture ELISA kit (Nordic Bioscience Diagnosis A/S).

Immunofluorescence and Confocal Microscopy—Osteoclasts grown on glass slides in a 24-well plate were fixed with 4% paraformaldehyde in PBS for 20 min, followed by permeabilization and blocking in PBS/0.2% BSA for 30 min. The cells were then incubated with primary antibodies in 0.2% BSA/PBS overnight at 4 °C. Primary antibody binding was visualized using fluorescent dye-conjugated secondary antibodies (Jackson ImmunoResearch Laboratories) in 0.2% BSA/PBS for 1 h. F-actin was stained with Alexa Fluor 488-phalloidin. Samples were mounted with 70% glycerol/PBS. Immunofluorescence-labeled cells were observed with a Carl Zeiss fluorescence microscope equipped with a CCD camera and analyzed using a Zeiss Spectral confocal laser scanning microscope equipped with Argon-Krypton lasers (LSM510 Zeiss Microsystems).

Dynamic Imaging of Osteoclasts—WT osteoclasts expressing PIP5Kγ1, PIP5Kγ2, and PIP5KIγ-KD, co-transduced with GFP-actin were maintained using standard culture conditions (37 °C and 5% CO_2, 95% air atmosphere) with RANKL and M-CSF, for 5 days, in a Bioptechs (non-liquid perfused) Delta T culture system, consisting of a heated, indium-tin-oxide-coated glass dish attached to a calibrated Bioptechs microperfusion peristaltic pump. All cultures were observed with a 20× objective (numerical aperture of 0.4) of an inverted automated wide field epifluorescence DIC microscope (Leica DMIRE2, Leica Microsystems, Wetzlar, Germany). An objective lens heater was used to improve temperature homogeneity. Images (608 × 512 pixels spatial and 12-bit intensity resolution) were recorded with a cooled Retiga 1300 camera (Qimaging, Burnaby, BC, Canada) every 2 min in 2 × 2 binned acquisition mode, using 100–300-ms exposures. Dynamic images were composed using NIH ImageJ software.

Histological Analysis of Mouse Pups—Embryonic bones were fixed in 10% formalin, and decalcified sections were stained for

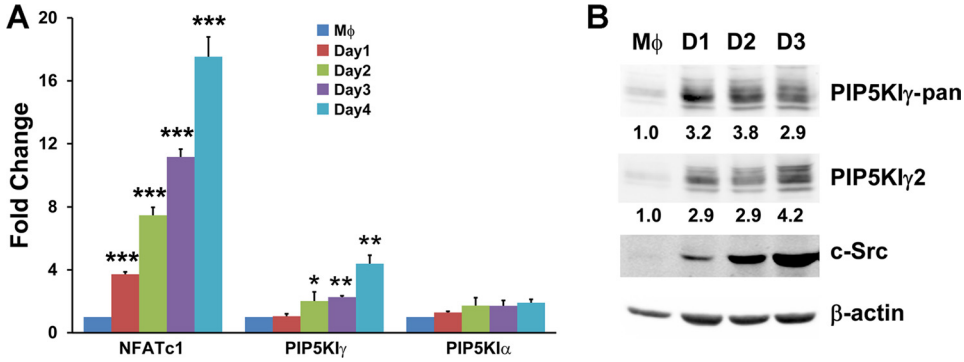

FIGURE 1. **PIP5KIγ expression increases with osteoclastogenesis.** *A*, WT BMMs were cultured with RANKL and M-CSF or M-CSF alone (Mϕ) for 4 days. PIP5KIγ and PIP5KIα mRNA was measured by quantitative PCR and normalized to Mϕ. NFATc1 mRNA, also normalized to Mϕ, serves as a marker of osteoclast differentiation (*, $p < 0.05$; **, $p < 0.01$; ***, $p < 0.001$). *B*, BMMs were cultured with RANKL and M-CSF or M-CSF alone (Mϕ) for 3 days. Total PIP5KIγ and PIP5KIγ2 were measured by immunoblot. c-Src serves as marker of osteoclast differentiation. β-Actin serves as loading control. *Numbers* represent densitometric analysis of PIP5KIγ/β-actin ratio normalized to that of Mϕ.

TRAP activity. Osteoclastic and perimeters were measured and analyzed using BioQuant OsteoII (BioQuant Image Analysis Corp., Nashville, TN) in a blinded fashion.

Statistics—All data are expressed as mean ± S.D., and statistical significance was calculated by analysis of variance.

RESULTS

PIP5KIγ Deficiency Inhibits Osteoclast Formation but Not Function—Our first exercise in exploring the role of PIP5KIγ in osteoclast formation and function was to determine the expression of the enzyme with precursor differentiation. PIP5KIγ mRNA, measured by quantitative PCR, was detectable in naïve BMMs and increased ~5-fold with exposure to the osteoclastogenic cytokines, whereas PIP5KIα mRNA did not change (Fig. 1*A*). M-CSF/RANKL-induced protein expression was as profound, enhancing total PIP5KIγ and PIP5KIγ2, 3.8- and 4.2-fold, respectively (Fig. 1*B*).

We next assessed the impact of PIP5KIγ on osteoclast formation. Because deletion of the kinase results in perinatal lethality, we utilized liver as the source of PIP5KIγ$^{-/-}$ and WT osteoclast precursors.

To generate osteoclasts, we exposed liver-derived macrophages to M-CSF and increasing amounts of RANKL for 4 days and stained them for TRAP activity. Osteoclasts of both genotypes increased progressively with RANKL dose (Fig. 2, *A* and *B*). In all circumstances, however, the number of polykaryons was significantly less in cultures containing PIP5KIγ$^{-/-}$ cells. This difference in osteoclastogenesis was most apparent at relatively low concentrations of the cytokine. The decreased number of mutant osteoclasts was reflected by diminished expression of the specific differentiation markers, β3 integrin subunit, NFATc1, and c-Src (Fig. 2*C*).

To determine the physiological relevance of the decreased osteoclastogenesis attending PIP5KIγ deficiency, *in vitro*, we asked whether the same obtains *in vivo*. Thus, we prepared histological sections of long bones of PIP5KIγ$^{-/-}$ and WT newborn mice and stained them for TRAP activity. In keeping with our *in vitro* observations, PIP5KIγ-deficient mice have a striking paucity of osteoclasts (Fig. 3).

These experiments indicate that PIP5KIγ is essential for generation of normal numbers of osteoclasts, *in vitro* and *in vivo*. In

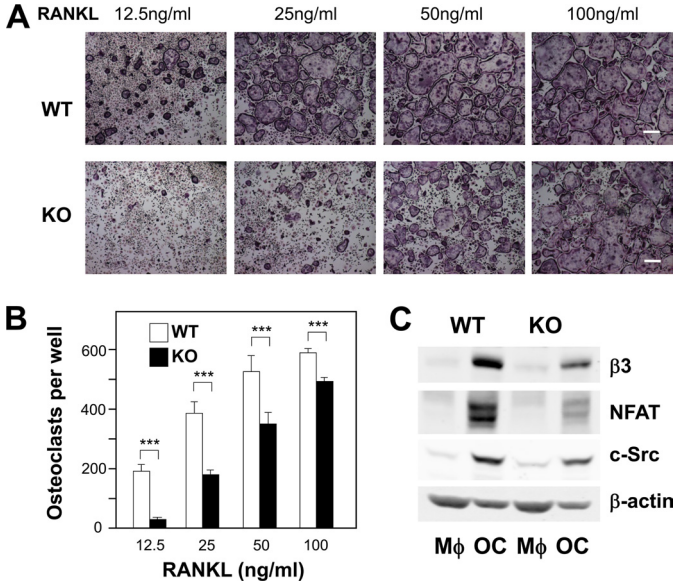

FIGURE 2. **PIP5KIγ deficiency inhibits osteoclastogenesis *in vitro*.** *A* and *B*, macrophages derived from 1-day-old WT or PIP5KIγ$^{-/-}$ (KO) mice liver were cultured in M-CSF (20 ng/ml) and increasing amounts of RANKL. After 4 days, the cells were stained for TRAP activity (*A*), and osteoclasts were counted (*B*; ***, $p < 0.001$). *Scale bar*, 250 μm. *C*, osteoclast differentiation markers β3-integrin, NFATc1, and c-Src, expressed by WT and PIP5KIγ$^{-/-}$ (KO) macrophages (*Mϕ*) and osteoclasts (*OC*) generated by 4-day exposure to RANKL and M-CSF, were determined by immunoblot. β-Actin serves as loading control.

both circumstances, however, the kinase-deficient TRAP-expressing polykaryons were well spread and morphologically identical to their WT counterparts, suggesting normal cytoskeletal organization and function. In keeping with this posture, actin ring formation by mutant or WT prefusion osteoclasts generated on bone was indistinguishable (supplemental Fig. 1*A*). To directly assess resorptive capacity of individual cells, prefusion osteoclasts were generated on plastic by 3 days exposure to RANKL and M-CSF, at which time proliferation is largely arrested. The cells were lifted and equal numbers placed on bone slices. Resorption pits, quantified 3 days later, were excavated in equal numbers by WT and PIP5KIγ$^{-/-}$ osteoclasts (supplemental Fig. 1, *B* and *C*).

PIP5KIγ Regulates RANKL Signaling—Because M-CSF and RANKL are necessary and sufficient for osteoclastogenesis, we asked which of these cytokines is impacted by absence of

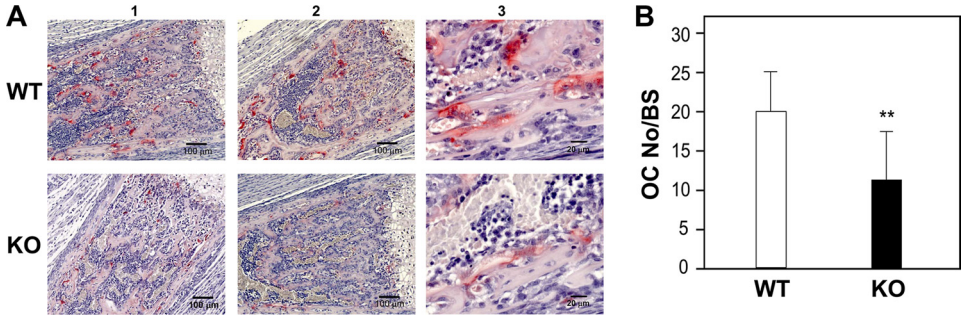

FIGURE 3. **PIP5KIγ deficiency inhibits osteoclastogenesis *in vivo*.** *A*, TRAP-stained (red reaction product) femurs of two WT and PIP5KIγ$^{-/-}$ (KO) newborn littermate pups demonstrating marked reduction of osteoclast abundance in mutant animals (*panels 1* and *2*). *Scale bar*, 100 μm. High magnification of WT and PIP5KIγ$^{-/-}$ (KO) osteoclasts shows that they are indistinguishable and juxtaposed to bone (*panel 3*). *Scale bar*, 20 μm. *B*, osteoclast number (*OC No*)/mm bone surface (*BS*) in femurs of WT and PIP5KIγ$^{-/-}$ newborn pups (**, $p < 0.01$).

PIP5KIγ. Thus, we treated WT and mutant liver-derived osteoclast precursors with either M-CSF or RANKL and assessed activation of established effector molecules, which mediate osteoclast formation. Absence of PIP5KIγ had no effect on M-CSF-induced phosphorylation of ERK, JNK, or AKT (Fig. 4*A*). The same cells exposed to RANKL, however, were incapable of normally activating AKT, JNK, or p38 (Fig. 4*B*). Because these data indicate RANKL mediates the osteoclastogenic properties of PIP5KIγ, we determined whether the cytokine activates the kinase? Thus, we transduced macrophages derived from PIP5KIγ$^{-/-}$ liver with HA-PIP5KIγ and exposed the cells to either of the two cytokines for as long as 15 min. HA immunoprecipitates were immunoblotted for tyrosine phosphorylation, a marker of the activation of the kinase (Fig. 4*C*). Consistent with induction of its effectors, RANKL, but not M-CSF, phosphorylates PIP5KIγ. The RANKL-induced calcium signal is essential for osteoclast differentiation. Because PIP5KIγ modulates calcium transport, which in turn, activates the key osteoclastogenic transcription factor, NFATc1, we asked if absence of the kinase disrupts calcium signaling in osteoclast precursors. Consistent with impaired osteoclastogenesis, RANKL-induced calcium signaling is diminished in PIP5KIγ$^{-/-}$ macrophages (Fig. 4, *D* and *E*). Thus, PIP5KIγ promotes osteoclast differentiation by sensitizing its precursors to RANKL.

PIP_2 Is Undetectable in PIP5KIγ$^{-/-}$ Osteoclast Precursors—To measure total PIP_2 in WT and PIP5KIγ$^{-/-}$ osteoclast precursors, we turned to high resolution ESI-MS. WT BMMs contain the doubly charged cluster ions of 18:0/20:4-PIP_2 at 522.2376 (calculated 522.2376) and 522.7390 (calculated 522.7393), and of 18:0/20:4-PI at *m*/*z* 885.5489 (calculated 885.5499). As shown in supplemental Fig. 2, the amount of the 18:0/20:4-PI species in WT (*top right panel*) and PIP5KIγ$^{-/-}$ (*bottom right panel*) BMMs is nearly identical. Although the 18:0/20:4-PIP_2 (monoisotopic ion seen at *m*/*z* 522.2376) in WT (*top left panel*) is of low abundance, the ion representing 18:0/20:4-PIP_2 is not observed in the PIP5KIγ$^{-/-}$ sample (*bottom left panel*) as evidenced by the absence of the expected m/z and isotopic pattern (the ion at *m*/*z* 522.2835 represents contamination). The results are consistent with the decreased levels of PIP_2 in the brain of the PIP5KIγ$^{-/-}$ mice (5, 17). Furthermore, given the specificity of PIP5KIγ in generating $PI(4,5)P_2$, these observations suggest it is the major PIP_2 in osteoclast precursors.

PIP5KIγ Excess Disrupts Osteoclast Formation and Function—With the expectation that PIP5KIγ1 or PIP5KIγ2 would rescue the osteoclastogenic failure of PIP5KIγ deficiency, we transduced WT constructs, tagged to HA, into mutant liver cells that were then cultured in M-CSF and RANKL for 4 days. Unexpectedly, osteoclast number of either PIP5KIγ$^{-/-}$ transductant did not increase and, in fact, decreased further relative to those bearing vector (Fig. 5, *A* and *B*). These observations raised the possibility that excess $PI(4,5)P_2$ synthesis may, similar to its deficiency, arrest osteoclastogenesis. This hypothesis is in keeping with the anti-osteoclastogenic effects of a likely cause of $PI(4,5)P_2$ accumulation, namely absence of phospholipase Cγ2, which also disrupts organization of the cytoskeleton of the cell (7, 8). In fact, while the magnitude of the 18:0/20:4-PIP_2 peak in empty vector-transduced BMMs is similar to that of WT, overexpressed PIP5KIγ1 and PIP5KIγ2 increases it by ~2 orders of magnitude (supplemental Table 1) and markedly alters the facade of PIP5KIγ$^{-/-}$ osteoclasts. Both transductants exhibit features common to osteoclasts incapable of normal cytoskeletal organization in that they fail to spread and have a "crenated" appearance (1). Confirming this phenomenon is talin-independent, PIP5IKγ2, but not PIP5KIγ1, binds to the integrin-activating protein in osteoclasts (Fig. 5*C*).

To determine the effect of increased PIP5KIγ on normal osteoclastogenesis, we transduced WT BMMs with PIP5KIγ1, PIP5KIγ2, or empty vector. Both splice variants delay osteoclast differentiation and disfigure the cell (Fig. 6, *A*–*C*). The magnitude of inhibited osteoclastogenesis and the distorted appearance of TRAP-expressing cells reflects the quantity of transduced PIP5KIγ (Fig. 6, *D* and *E*). Furthermore, in control WT osteoclasts, PIP5KIγ localizes with actin in podosome belts (Fig. 6*F*). Overexpressed PIP5KIγ2 and PIP5KIγ1 also co-localize with actin but not in podosome belts as these structures fail to form, thereby confirming cytoskeletal impairment (supplemental Movie 1). Thus, a surfeit of PIP5KIγ disrupts formation of osteoclasts and organization of their cytoskeleton.

The multifunctional properties of PIP5KIγ reflect the fact that it serves as both a kinase and adaptor protein. We, therefore, asked whether the inhibitory properties of the molecule require its enzymatic activity. Transduction of a kinase-inactive PIP5KIγ mutant (PIP5KIγ-KD), incapable of catalyzing $PI(4,5)P_2$ synthesis, yielded normal appearing WT osteoclasts with podosome belts and did not suppress their number (Fig. 6, *A* and *B*, supplemental Movie 2). This observation is fortified by

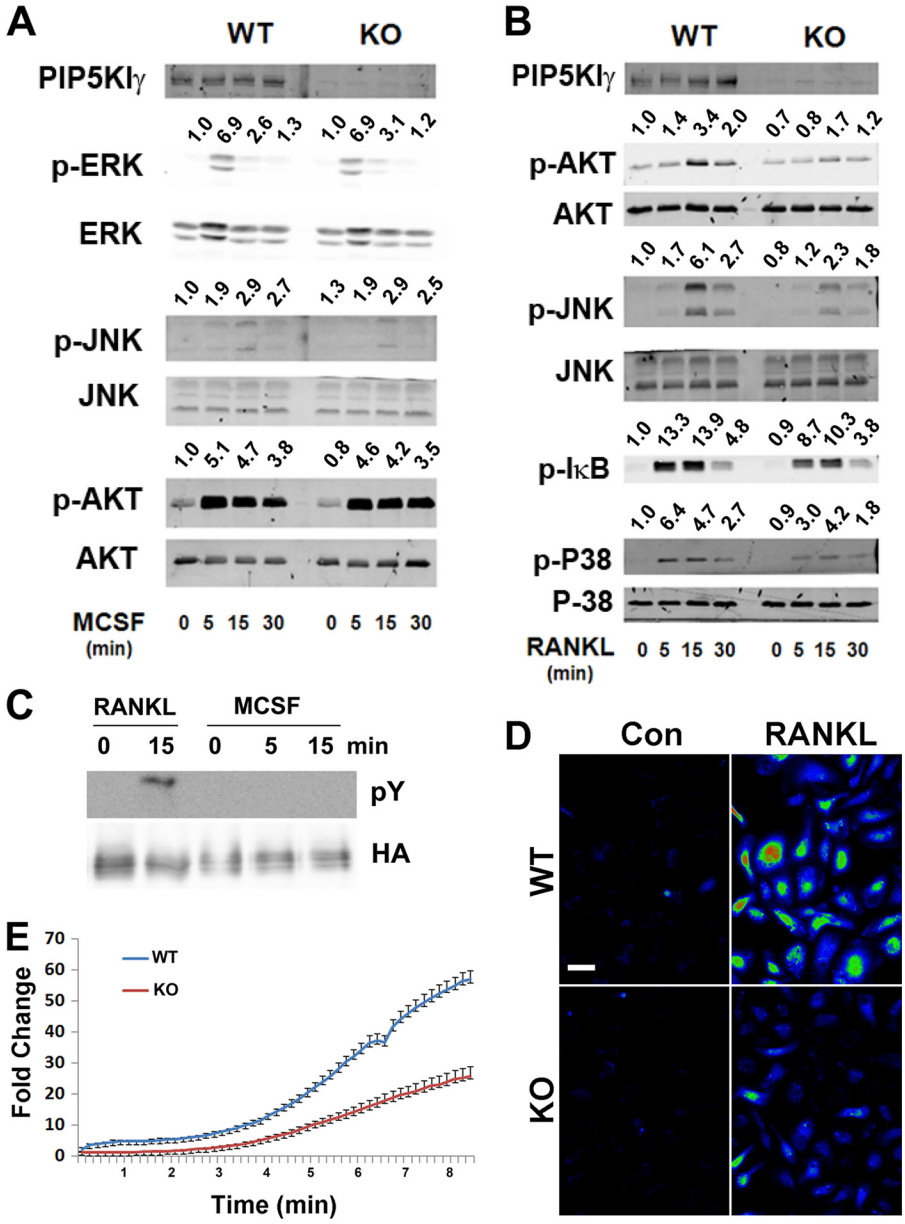

FIGURE 4. **PIP5KIγ deficiency regulates RANKL-induced signaling in osteoclast precursors.** *A*, serum- and cytokine-starved WT and PIP5KIγ$^{-/-}$ (KO) macrophages were exposed to M-CSF (100 ng/ml). Phosphorylated and total AKT, ERK, and JNK were immunoblotted with time. Total relevant proteins serve as loading control. *B*, serum- and cytokine-starved WT and PIP5KIγ$^{-/-}$ (KO) macrophages were exposed to RANKL (100 ng/ml) Phosphorylated and total AKT, JNK, IkB, and p38 were immunoblotted with time. Total relevant proteins serve as loading controls. *C*, PIP5KIγ$^{-/-}$ liver cells, transduced with HA-PIP5KIγ2, were stimulated by RANKL (100 ng/ml) and M-CSF (100 ng/ml) for as long as 15 min. HA immunoprecipitates were immunoblotted with anti-phosphotyrosine mAb. *D*, WT and PIP5KIγ$^{-/-}$ BMMs, stained with Flur-4, were stimulated with RANKL (200 ng/ml). $[Ca^{2+}]_i$ was imaged prior to con and 8 min after RANKL exposure. *Scale bar*, 25 μm. *E*, average increase in $[Ca^{2+}]_i$ during stimulation with RANKL in WT and PIP5KIγ-deficient BMMs.

failure of PIP5KIγ-KD to dampen expression of differentiation markers of WT osteoclast precursors cultured with RANKL or M-CSF or to reduce RANKL-stimulated NFATc1 nuclear translocation (Fig. 6, *G* and *H*).

To explore the functional implications of excess PIP5KIγ, we assessed the bone-degrading capacity of osteoclasts transduced with either isoform as well as that lacking kinase activity. Overexpressed PIP5KIγ2 or particularly PIP5KIγ1 substantially reduces resorptive pit formation and CTx mobilization, which does not occur absent kinase activity (Fig. 7, *A–C*). To determine whether the diminished resorption reflects impaired capacity of individual cells as well as a reduction in their number, we cultured transduced BMMs in M-CSF and RANKL for 5 days on Petri dish at which time they are committed to the osteoclast phenotype. The cells were lifted, and equal numbers placed on bone slices for 2 days. Again, excess PIP5KIγ1 or PIP5KIγ2 impairs pit formation (Fig. 7*D*). Because the lifted cells are no longer replicative, this experiment establishes that dysfunction of the individual osteoclast contributes to the attenuated resorption induced by PIP5KIγ excess.

DISCUSSION

$PI(4,5)P_2$ comprises a minor component of membrane phospholipids but profoundly influences the function of all cells. It

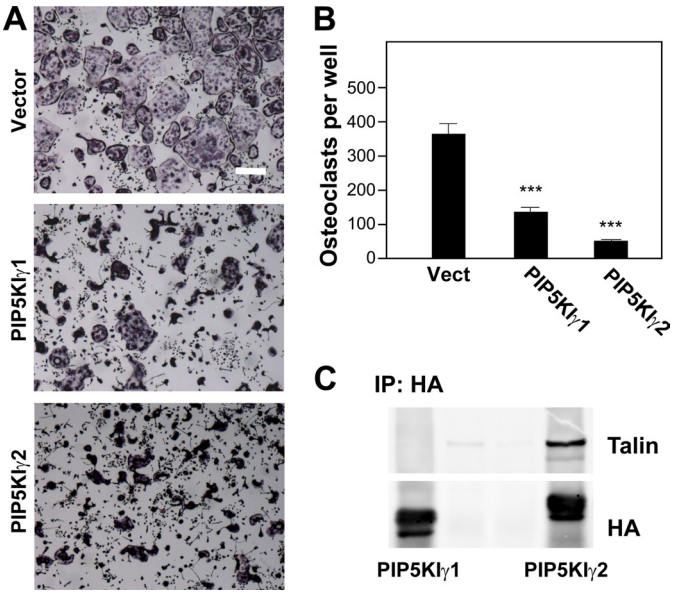

FIGURE 5. **PIP5KIγ overexpression arrests osteoclast formation and cytoskeletal organization.** *A* and *B*, PIP5KI$\gamma^{-/-}$ liver cells, transduced with HA-PIP5KIγ1, HA-PIP5KIγ2, or empty vector (*Vect*), were cultured with RANKL and M-CSF for 4 days. The cells were stained for TRAP activity (*A*), and osteoclasts were counted (*B*; ***, $p < 0.001$). *Scale bar*, 250 μm. *C*, HA immunoprecipitates of PIP5KI$\gamma^{-/-}$ cells transduced with HA-PIP5KIγ1 or HA-PIP5KIγ2 were immunoblotted with anti-talin or anti-HA mAb.

serves not only as precursor to second messengers, but the intact PI is an important signaling molecule in its own right. Osteoclasts increase in number in mice lacking the 5′ lipid phosphatase, SHIP1, due to cell cycle activation of their precursors (23). SHIP1$^{-/-}$ BMMs are also hypersensitive to RANKL and M-CSF and, in consequence, generate large, active osteoclasts resulting in severe osteoporosis (24). Additionally, PI(4,5)P_2 and PIP_3 interact with gelsolin, thereby regulating podosome assembly and signaling in the bone resorptive cell (3, 25). Finally, phospholipase Cγ2, which metabolizes PI(4,5)P_2 to diacylglycerol and PIP_3, modulates osteoclast formation and function (7, 8).

The PIP5KI family, which accounts for the majority of PI(4,5)P_2 synthesis, consists of α, β and γ isoforms which distribute in distinct intracellular locations and thus appear to regulate individual biological events. Because osteoclast function is attended by dramatic cytoskeletal reorganization, which in other cells is regulated by PIP5KIγ, we reasoned that deletion of this isoform is most likely to impact the resorptive cell (9, 11, 17, 18). Our finding that PIP5KIγ2 increases in abundance as macrophages commit to the osteoclast phenotype fortifies this hypothesis. To determine whether the enzyme is necessary for osteoclast formation or function, we utilized mice globally deleted of all splice variants of PIP5KIγ. Because these animals die perinatally, we generated osteoclasts by culturing macrophage-containing hepatic aspirates in M-CSF and RANKL.

In keeping with the role of PIs in cell maturation, absence of PIP5KIγ delays osteoclast differentiation, particularly that induced by relatively modest amounts of RANKL. Importantly, the requirement for PIP5KIγ in skeletal metabolism is established by the paucity of osteoclasts in mice lacking the kinase.

As in the case of phospholipase Cγ2 deficiency, osteoclastic cells lacking PIP5KIγ respond normally to M-CSF but not RANKL (7). In both conditions, there is dampened activation and expression of osteoclast differentiation markers, including NFAT, which in other cells is regulated by diacylglycerol and PIP_3 (11). The blunted osteoclastogenesis of PIP5KIγ- and phospholipase Cγ2-deficient osteoclasts is consistent with the expected reduction of PI(4,5)P_2 metabolites in both circumstances. Furthermore, as SHIP1 deficiency, which is attended by increased PIP_3 expression (26), is characterized by enhanced osteoclastogenesis, the reduced numbers of PIP5KI$\gamma^{-/-}$ osteoclasts may reflect arrest of a second metabolic event whereby PI(4,5)P_2 is phosphorylated to PIP_3 by PI3K (27).

In contrast, PIP5KI$\gamma^{-/-}$ osteoclasts exhibit no apparent cytoskeletal abnormalities. The cells spread as effectively as their WT counterparts, they form actin rings, and the individual bone resorbing capacities of both genotypes are indistinguishable. This observation is surprising as PI(4,5)P_2 regulates many aspects of cytoskeletal function in other cells and is purported to do so in the osteoclast (3). Furthermore, PIP5KIγ2 resides within focal adhesions and interacts with structural proteins such as talin, facilitating its association with integrins. Talin/integrin binding is a necessary event whereby these heterodimers organize the cytoskeleton, including that of osteoclasts (13, 14, 28). As most cells possess more than one isoform of PIP5KI, which may in some circumstances be redundant, a reasonable, albeit speculative, hypothesis holds that PIP5Kα and/or PIP5Kβ prevent osteoclast dysfunction in face of PIP5Kγ deficiency (11, 18). This posture is challenged, however, by the absence of MS-detectable PIP_2 in PIP5K$\gamma^{-/-}$ osteoclast precursors in the form of BMMs.

In contrast to the normal appearance of individual bone resorptive cells lacking PIP5KIγ, its overexpression in mutant or WT cells inhibits spreading and yields a "pyknotic" appearance common to osteoclasts with disorganized cytoskeletons (1). The abnormal cytoskeleton attending excess PIP5KγI is not unique to osteoclasts as focal adhesions are disrupted in other cells overexpressing the kinase (9, 29). The mechanism of inhibited cytoskeletal organization, in these circumstances, is unknown but postulated to reflect local disruption of PI balance and removal of talin from focal adhesions by PIP5KIγ2 (9, 13, 14).

Our results indicate that the mechanisms of cytoskeletal dysfunction in PIP5KI-overexpressing osteoclasts may differ from those previously reported in other cells. Specifically, we find that cytoskeletal distortion occurs with equal efficiency in those bearing either PIP5KIγ2, which binds talin and removes it from focal adhesions, or PIP5KIγ1, which does not. Transduction of either splice variant fails to rescue the anti-osteoclastogenic effects of PIP5KI depletion, but this likely reflects abundance of the overexpressed proteins. Excess PIP5KIγ1 or PIP5KIγ2 mirrors absence of the parent gene, which arrests osteoclast formation due to delayed differentiation, but the overexpressed proteins also disrupt the cytoskeleton. The reduced number of osteoclasts in PIP5KIγ-transduced WT cells, in combination with the disruptive cytoskeletal effects, substantially dampens resorption. Similar to cytoskeletal organization, the diminished osteoclast abundance attending PIP5KIγ excess reflects intact enzymatic activity as it does not occur in cells bearing a kinase-arrested mutant.

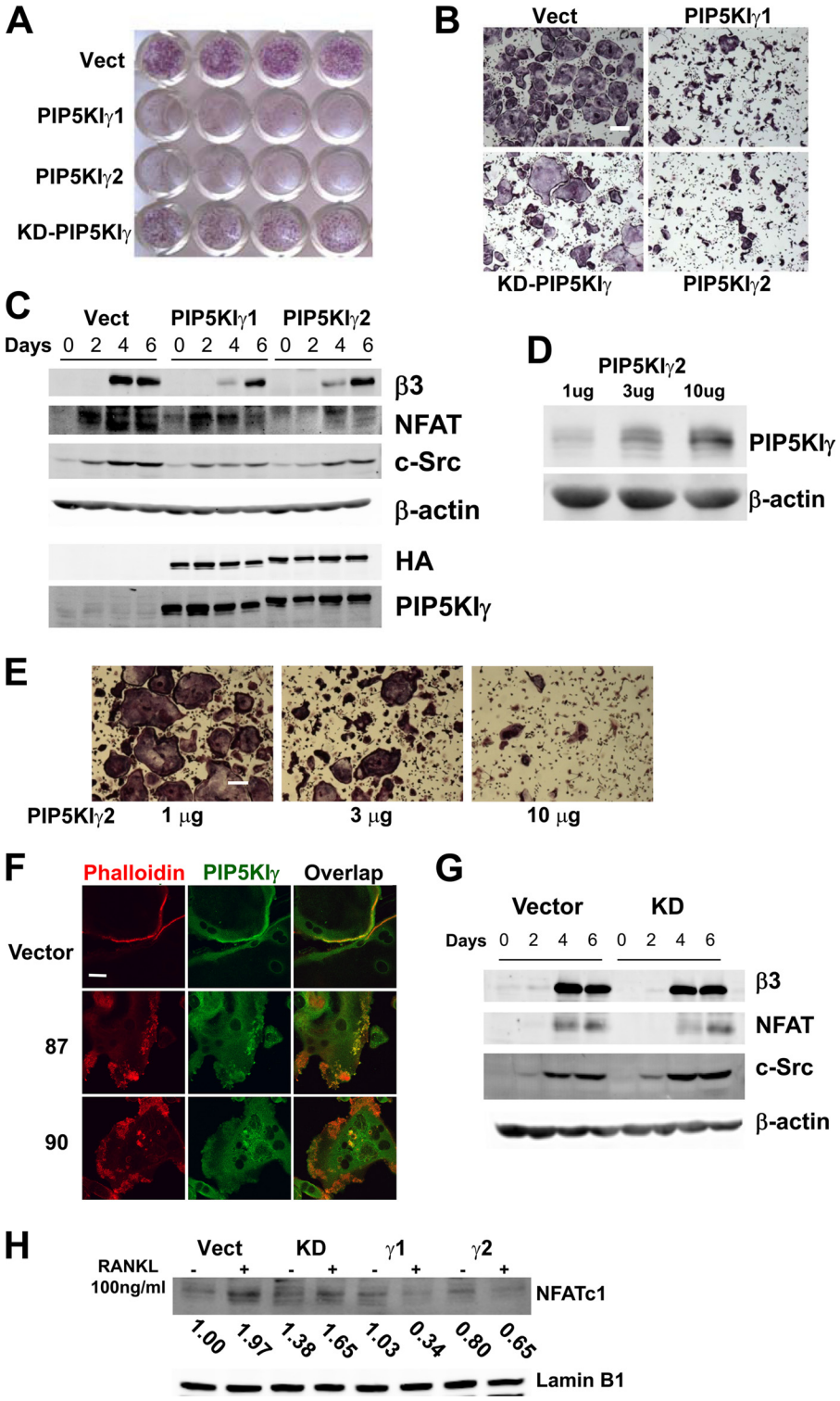

FIGURE 6. **PIP5KIγ1 or PIP5KIγ2 overexpression arrests WT osteoclast formation and cytoskeletal organization in a kinase-dependent manner.** *A*, WT BMMs transduced with vector, PIP5KIγ1, PIP5KIγ2, or kinase-inactive PIP5KIγ (PIP5KIγ-KD) were cultured with RANKL and M-CSF for 4 days. The cells were stained for TRAP activity. *B*, appearance of cells as described in *A*. *Scale bar*, 250 μm. *C*, WT BMMs transduced with HA-PIP5KIγ1, HA-PIP5KIγ2, or vector were exposed to M-CSF and RANKL. Markers of osteoclast differentiation, HA, and PIP5KIγ were immunoblotted. β-Actin serves as loading control. *D*, WT BMMs were transduced with increasing amounts of PIP5KIγ2 plasmid, and expression was determined by immunoblot. β-Actin serves as loading control. *E*, WT BMMs transduced with increasing amounts of PIP5KIγ2 plasmid were cultured with RANKL and M-CSF for 4 days. The cells were stained for TRAP activity. *Scale bar*, 250 μm. *F*, WT osteoclasts transduced with PIP5KIγ1, PIP5KIγ2, or vector (*Vect*) were stained with anti-PIP5KIγ mAb (*green*) or phalloidin (*red*) to identify fibrillar actin. The kinase localizes with actin in peripheral podosome belts in vector-transduced cells (*yellow*). No podosome belts form in PIP5KIγ1- and PIP5KIγ2-transduced osteoclasts, although kinase/actin co-localization is evident in other locations. *Scale bar*, 25 μm. *G*, WT BMMs, transduced with vector or PIP5KIγ-KD, were cultured in M-CSF and RANKL. Markers of osteoclast differentiation were immunoblotted with time. β-Actin serves as loading control. *H*, WT preosteoclasts transduced with vector, PIP5KIγ1, PIP5KIγ2, or PIP5KIγ-KD were treated with RANKL for 20 min. Nuclear proteins were extracted and immunoblotted by NFATc1. The nuclear protein, lamin B1, serves as loading control.

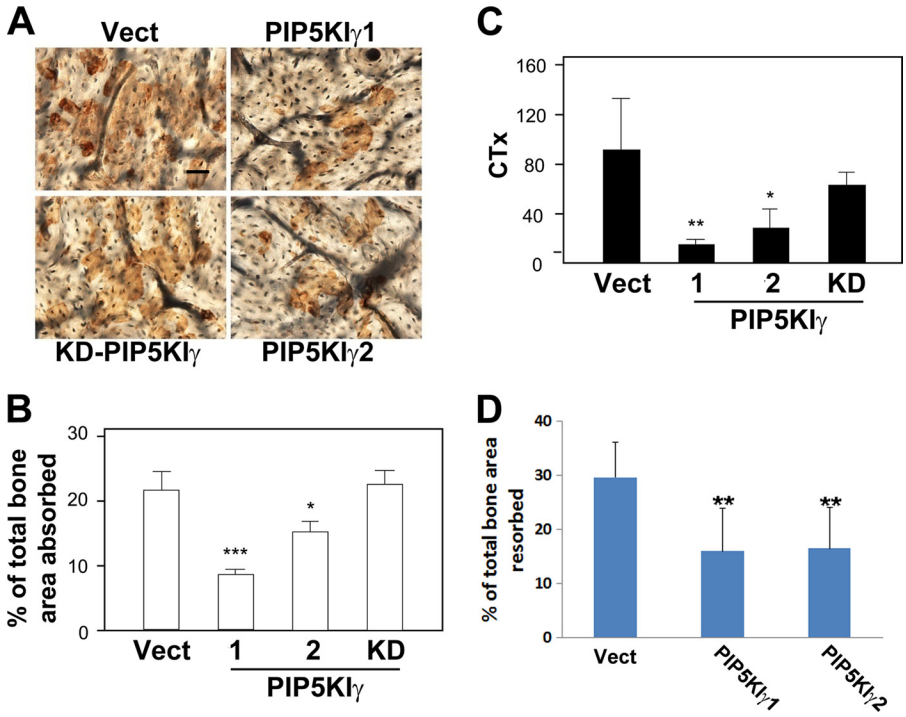

FIGURE 7. **Excess PIP5Kγ impairs bone resorption.** *A–C*, WT BMMs transduced with vector (*Vect*), PIP5KIγ1, PIP5KIγ2, or PIP5KIγ-KD were cultured on bone slices in the presence of RANKL and M-CSF. *A*, after 6 days, the cells were removed, and resorption pits were visualized by peroxidase-labeled wheat germ agglutinin (brown reaction product) (200×). *Scale bar*, 50 μm. *B*, quantification of area of bone resorbed. *C*, carboxyl-terminal collagen cross-links (*CTx*) concentration in culture medium as determined by ELISA. *D*, PIP5KIγ1, PIP5KIγ2, or vector-transduced BMMs were cultured on Petri dish for 5 days with M-CSF and RANKL. The cells were lifted, and equal numbers were placed on bone slices. Bone resorptive pits were visualized, and the resorptive area quantified 2 days later (*, $p < 0.05$; **, $p < 0.01$; ***, $p < 0.001$).

As overexpressed PIP5KIγ enhances $PI(4,5)P_2$ generation, our data raise the possibility that this PI, in excess, attenuates osteoclastogenesis and disrupts the cytoskeleton of the cell. These observations are in keeping with impairment of osteoclast formation and cytoskeletal organization attending deficient phospholipase Cγ2 activity (7), another state of $PI(4,5)P_2$ abundance (9). Thus, both insufficient and excess PIP5KIγ impact the osteoclast. Absence of the enzyme compromises its differentiation but not its function, whereas excess kinase disrupts both. These observations indicate that optimal amounts of PIP5KIγ and its metabolites are essential for skeletal homeostasis.

Acknowledgment—We thank Dr. Richard A. Anderson (University of Wisconsin) for providing PIP5Kγ antibody.

REFERENCES

1. Teitelbaum, S. L. (2007) Osteoclasts: what do they do and how do they do it? *Am. J. Pathol.* **170,** 427–435
2. Biswas, R. S., Baker, D., Hruska, K. A., and Chellaiah, M. A. (2004) Polyphosphoinositides-dependent regulation of the osteoclast actin cytoskeleton and bone resorption. *BMC Cell Biol.* **5,** 19
3. Chellaiah, M. A. (2006) Regulation of podosomes by integrin αvβ3 and Rho GTPase-facilitated phosphoinositide signaling. *Eur. J. Cell Biol.* **85,** 311–317
4. Mao, Y. S., and Yin, H. L. (2007) Regulation of the actin cytoskeleton by phosphatidylinositol 4-phosphate 5 kinases. *Pflügers Arch.* **455,** 5–18
5. van den Bout, I., and Divecha, N. (2009) PIP5K-driven PtdIns(4,5)P2 synthesis: regulation and cellular functions. *J. Cell Sci.* **122,** 3837–3850
6. Faccio, R., and Cremasco, V. (2010) PLCγ2: where bone and immune cells find their common ground. *Ann. N.Y. Acad. Sci.* **1192,** 124–130
7. Mao, D., Epple, H., Uthgenannt, B., Novack, D. V., and Faccio, R. (2006) PLCg2 regulates osteoclastogenesis via its interaction with ITAM proteins and GAB2. *J. Clin. Invest.* **116,** 2869–2879
8. Epple, H., Cremasco, V., Zhang, K., Mao, D., Longmore, G. D., and Faccio, R. (2008) Phospholipase Cγ2 modulates integrin signaling in the osteoclast by affecting the localization and activation of Src kinase. *Mol. Cell Biol.* **28,** 3610–3622
9. Scott, C. C., Dobson, W., Botelho, R. J., Coady-Osberg, N., Chavrier, P., Knecht, D. A., Heath, C., Stahl, P., and Grinstein, S. (2005) Phosphatidylinositol-4,5-bisphosphate hydrolysis directs actin remodeling during phagocytosis. *J. Cell Biol.* **169,** 139–149
10. Ishihara, H., Shibasaki, Y., Kizuki, N., Wada, T., Yazaki, Y., Asano, T., and Oka, Y. (1998) Type I phosphatidylinositol-4-phosphate 5-kinases. Cloning of the third isoform and deletion/substitution analysis of members of this novel lipid kinase family. *J. Biol. Chem.* **273,** 8741–8748
11. Mao, Y. S., Yamaga, M., Zhu, X., Wei, Y., Sun, H. Q., Wang, J., Yun, M., Wang, Y., Di Paolo, G., Bennett, M., Mellman, I., Abrams, C. S., De Camilli, P., Lu, C. Y., and Yin, H. L. (2009) Essential and unique roles of PIP5K-γ and -α in Fcγ receptor-mediated phagocytosis. *J. Cell Biol.* **184,** 281–296
12. Wang, Y. J., Li, W. H., Wang, J., Xu, K., Dong, P., Luo, X., and Yin, H. L. (2004) Critical role of PIP5KIγ87 in InsP3-mediated Ca^{2+} signaling. *J. Cell Biol.* **167,** 1005–1010
13. Di Paolo, G., Pellegrini, L., Letinic, K., Cestra, G., Zoncu, R., Voronov, S., Chang, S., Guo, J., Wenk, M. R., and De Camilli, P. (2002) Recruitment and regulation of phosphatidylinositol phosphate kinase type 1γ by the FERM domain of talin. *Nature* **420,** 85–89
14. Ling, K., Doughman, R. L., Firestone, A. J., Bunce, M. W., and Anderson, R. A. (2002) Type I γ phosphatidylinositol phosphate kinase targets and regulates focal adhesions. *Nature* **420,** 89–93
15. Zou, W., Izawa, T., Zhu, T., Chappel, J., Otero, K., Monkley, S. J., Critchley, D. R., Petrich, B. G., Morozov, A., Ginsberg, M. H., and Teitelbaum, S. L. (2012) Talin1 and Rap1 are Critical for Osteoclast Function. *Mol. Cell Biol.* [Epub ahead of print]
16. Zhao, H., Ito, Y., Chappel, J., Andrews, N. W., Teitelbaum, S. L., and Ross,

F. P. (2008) Synaptotagmin VII regulates bone remodeling by modulating osteoclast and osteoblast secretion. *Dev. Cell* **14,** 914–925
17. Di Paolo, G., Moskowitz, H. S., Gipson, K., Wenk, M. R., Voronov, S., Obayashi, M., Flavell, R., Fitzsimonds, R. M., Ryan, T. A., and De Camilli, P. (2004) Impaired PtdIns(4,5)P2 synthesis in nerve terminals produces defects in synaptic vesicle trafficking. *Nature* **431,** 415–422
18. Wang, Y., Litvinov, R. I., Chen, X., Bach, T. L., Lian, L., Petrich, B. G., Monkley, S. J., Kanaho, Y., Critchley, D. R., Sasaki, T., Birnbaum, M. J., Weisel, J. W., Hartwig, J., and Abrams, C. S. (2008) Loss of PIP5KIγ, unlike other PIP5KI isoforms, impairs the integrity of the membrane cytoskeleton in murine megakaryocytes. *J. Clin. Invest.* **118,** 812–819
19. Zou, W., Kitaura, H., Reeve, J., Long, F., Tybulewicz, V. L., Shattil, S. J., Ginsberg, M. H., Ross, F. P., and Teitelbaum, S. L. (2007) Syk, c-Src, the avb3 integrin, and ITAM immunoreceptors, in concert, regulate osteoclastic bone resorption. *J. Cell Biol.* **176,** 877–888
20. Faccio, R., Zou, W., Colaianni, G., Teitelbaum, S. L., and Ross, F. P. (2003) High dose M-CSF partially rescues the Dap12-/- osteoclast phenotype. *J. Cell Biochem.* **90,** 871–883
21. Wenk, M. R., Pellegrini, L., Klenchin, V. A., Di Paolo, G., Chang, S., Daniell, L., Arioka, M., Martin, T. F., and De Camilli, P. (2001) PIP kinase Iγ is the major PI(4,5)P(2) synthesizing enzyme at the synapse. *Neuron* **32,** 79–88
22. Pettitt, T. R., Dove, S. K., Lubben, A., Calaminus, S. D., and Wakelam, M. J. (2006) Analysis of intact phosphoinositides in biological samples. *J. Lipid Res.* **47,** 1588–1596
23. Zhou, P., Kitaura, H., Teitelbaum, S. L., Krystal, G., Ross, F. P., and Takeshita, S. (2006) SHIP1 negatively regulates proliferation of osteoclast precursors via Akt-dependent alterations in D-type cyclins and p27. *J. Immunol.* **177,** 8777–8784
24. Takeshita, S., Namba, N., Zhao, J. J., Jiang, Y., Genant, H. K., Silva, M. J., Brodt, M. D., Helgason, C. D., Kalesnikoff, J., Rauh, M. J., Humphries, R. K., Krystal, G., Teitelbaum, S. L., and Ross, F. P. (2002) SHIP-deficient mice are severely osteoporotic due to increased numbers of hyper-resorptive osteoclasts. *Nat. Med.* **8,** 943–949
25. Raucher, D., Stauffer, T., Chen, W., Shen, K., Guo, S., York, J. D., Sheetz, M. P., and Meyer, T. (2000) Phosphatidylinositol 4,5-bisphosphate functions as a second messenger that regulates cytoskeleton-plasma membrane adhesion. *Cell* **100,** 221–228
26. Sly, L. M., Ho, V., Antignano, F., Ruschmann, J., Hamilton, M., Lam, V., Rauh, M. J., and Krystal, G. (2007) The role of SHIP in macrophages. *Front. Biosci.* **12,** 2836–2848
27. Kang, H., Chang, W., Hurley, M., Vignery, A., and Wu, D. (2010) Important roles of PI3Kγ in osteoclastogenesis and bone homeostasis. *Proc. Natl. Acad. Sci. U.S.A.* **107,** 12901–12906
28. Halstead, J. R., Savaskan, N. E., van den Bout, I., Van Horck, F., Hajdo-Milasinovic, A., Snell, M., Keune, W. J., Ten Klooster, J. P., Hordijk, P. L., and Divecha, N. (2010) Rac controls PIP5K localisation and PtdIns(4,5)P synthesis, which modulates vinculin localisation and neurite dynamics. *J. Cell Sci.* **123,** 3535–3546
29. Weinkove, D., Bastiani, M., Chessa, T. A., Joshi, D., Hauth, L., Cooke, F. T., Divecha, N., and Schuske, K. (2008) Overexpression of PPK-1, the *Caenorhabditis elegans* Type I PIP kinase, inhibits growth cone collapse in the developing nervous system and causes axonal degeneration in adults. *Dev. Biol.* **313,** 384–397